Nondestructive crack detection in metal structures using impedance responses and artificial neural networks

Duc-Duy Ho[*1,2], Tran-Huu-Tin Luu [2,3a] and Minh-Nhan Pham [1,2b]

[1] *Faculty of Civil Engineering, Ho Chi Minh City University of Technology (HCMUT),
268 Ly Thuong Kiet Street, District 10, Ho Chi Minh City, Vietnam*
[2] *Vietnam National University Ho Chi Minh City, Linh Trung Ward, Thu Duc City, Ho Chi Minh City, Vietnam*
[3] *Vietnam National University Ho Chi Minh City, Campus in Ben Tre, Ben Tre, Vietnam*

Abstract. Among nondestructive damage detection methods, impedance-based methods have been recognized as an effective technique for damage identification in many kinds of structures. This paper proposes a method to detect cracks in metal structures by combining electro-mechanical impedance (EMI) responses and artificial neural networks (ANN). Firstly, the theories of EMI responses and impedance-based damage detection methods are described. Secondly, the reliability of numerical simulations for impedance responses is demonstrated by comparing to pre-published results for an aluminum beam. Thirdly, the proposed method is used to detect cracks in the beam. The RMSD (root mean square deviation) index is used to alarm the occurrence of the cracks, and the multi-layer perceptron (MLP) ANN is employed to identify the location and size of the cracks. The selection of the effective frequency range is also investigated. The analysis results reveal that the proposed method accurately detects the cracks' occurrence, location, and size in metal structures.

Keywords: artificial neural network; crack; damage detection; electro-mechanical impedance; structural health monitoring

1. Introduction

The problem of civil infrastructure occurring various types of damage in the operation process is inevitable. Structural health monitoring (SHM) is an essential target for the service life, safety, and sustainable development of the structures. The early warning of structural damages is essential when the damages are just formed, not when the damages are severe leading to structural failure. One of the methods to ensure the safety and integrity of structures is to regularly monitor the structural health so that the damages can be detected promptly and accurately. In the last few decades, research on SHM has mainly focused on structural response analysis, development of measurement techniques, development of structural damage identification methods, and practical applications (Farrar 2001, Li *et al*. 2014). Especially in industry 4.0, the application of artificial intelligence in the field of SHM is becoming more and more popular (Avci *et al*. 2021). On that

---

∗Corresponding author, Professor, E-mail: hoducduy@hcmut.edu.vn
[a] Master, E-mail: lthtin@vnuhcm.edu.vn
[b] Master Student, E-mail: pmnhan.sdh20@hcmut.edu.vn

basis, this paper focused on the structural damage detection method using electro-mechanical impedance responses combined with artificial neural network.

In recent years, various nondestructive crack detection techniques have been proposed for monitoring infrastructure. Yao *et al*. (2014) summarized the knowledge about cracking and its sources, reviewed both existing and emerging techniques for crack detection and characterization, and identified the advantages and challenges for these techniques. The study identified two sensing approaches (direct and indirect) and two data analysis approaches (model-based and model-free) along with a range of associated technologies. The advantages and challenges of each technique were discussed and summarized, and the future research needs were also identified. Zuo *et al*. (2017) developed a modified electro-mechanical impedance technique for crack detection that involves fusing information from multiple sensors. A new damage-sensitive feature factor based on a pipeline impedance model that considered the influence of the bonding layer between the sensors and pipeline was derived. The effectiveness of the proposed method was experimentally validated. A damage index, RMSD (root mean square deviation), was used to examine the degree and position of crack damage in a pipeline. Rao *et al*. (2021) proposed an automated detection method, which is based on convolutional neural network models and a non-overlapping window-based approach, to detect crack/non-crack conditions of concrete structures from images. The proposed approach provided over 95% accuracy and over 87% precision in detecting the cracks for most of the convolutional neural network models. The study showed that deeper convolutional neural network models had higher detection accuracies; however, they also required more parameters and had higher inference time.

Impedance-based SHM methods have been developed and widely applied in fields such as civil engineering, mechanical engineering, and aerospace engineering (Liang *et al*. 1994, Sun *et al*. 1995, Park *et al*. 2003, Min *et al*. 2012, Huynh *et al*. 2017, Ho *et al*. 2021, Fan *et al*. 2021). This non-destructive testing technique relies on the variation of the EMI responses measured from the PZT (lead zirconate titanate) sensor, which is bonded to the host structure. The PZT sensor's electrical impedance responses are related to the mechanical impedance responses of the structure. The PZT sensor's size and mass are tiny compared to the structure. Therefore, the PZT sensor will not affect the dynamic characteristics of the structure. The main principle of the impedance-based SHM method is to monitor the change in the mechanical impedance of the structure when the damages occur. This method is very effective for detecting the damages in local areas because it is sensitive to damages. Liang *et al*. (1994) first introduced the damage detection method using impedance. After that, many researchers have improved and applied the impedance-based SHM method for many different types of structures. Sun *et al*. (1995) presented the RMSD index of impedance responses for alarming the occurrence of damage. The impedance-based SHM method has been successfully applied to truss structures (Sun *et al*. 1995), thin sheet structures (Giurgiutiu and Zagrai 2005), reinforced concrete structures (Park *et al*. 2006, Ai *et al*. 2018), steel structures (Min *et al*. 2012, Ryu *et al*. 2017). Ho *et al*. (2014) evaluated the feasibility of numerical simulation of impedance-based damage detection in steel column connection. Therein, a numerical simulation of the impedance-based damage monitoring was performed for a steel column connection in which connection bolts were loosened.

An artificial neural network (ANN) is an information processing model that simulates the activity of an organism's neural network system, consisting of a large number of neurons connected to information processing. A large number of elements (neurons) are connected through links as a unified whole to handle and solve problems. An ANN is used to solve specific problems (data classification, pattern recognition, ...) through a learning process from a set of training

samples. In essence, learning is the process of adjusting the weights of connections between neurons (Lee *et al*. 2005). Recently, the combination of impedance-based methods and deep learning for SHM has been developed. Nguyen *et al*. (2022) proposed a convolutional neural network (CNN)-based autonomous feature extraction approach for impedance-based SHM. The proposed approach successfully estimated the actual severity of prestress-loss in the girder, even for untrained prestress cases.

Stemming from practical requirements and inheriting results from previous studies, this study's main objective is to detect cracks in metal structures using impedance responses combined with ANN taking into account the sensitivity of frequency range. The following contents are carried out in this study. First, the theories of EMI responses, damage detection method based on impedance response change, and artificial neural network are presented. Next, the method's feasibility is verified by numerical simulations on an aluminum beam. The numerical results are compared to pre-published ones. Finally, the cracks' occurrence, location, and size in the aluminum beam are identified using the proposed method.

2. Crack detection method using impedance responses and artificial neural networks

2.1 Electro-mechanical impedance responses

Recently, piezoelectric materials have been commonly used in the field of SHM. The advantages of piezoelectric materials are that they are light, cheap, versatile, and available in various shapes. The electro-mechanical impedance responses are based on a combination of mechanical and electrical properties of the material (Liang *et al*. 1994). The electro-mechanical interaction between the target structure and the PZT sensor is shown in Fig. 1. The structure is characterized by properties such as mass, stiffness, damping coefficients, and boundary conditions. Meanwhile, the PZT sensor is defined as an electrical circuit with harmonic amperage $I(\omega)$ and voltage $V(\omega)$.

The electro-mechanical impedance $Z(\omega)$, which is a function of the target structure's mechanical impedance $Z_s(\omega)$ and the PZT sensor's impedance $Z_a(\omega)$, is defined as follows

$$Z(\omega) = \left[j\omega \frac{w_p l_p}{t_p} \left(\left(\overline{\varepsilon_{33}^T} - d_{31}^2 \overline{Y_{11}^E} \right) + \frac{Z_a(\omega)}{Z_a(\omega) + Z_s(\omega)} d_{31}^2 \overline{Y_{11}^E} \left(\frac{\tan k\, l_p}{k l_p} \right) \right) \right]^{-1} \tag{1}$$

where $\overline{\varepsilon_{33}^T}$ is the complex electric permittivity at constant stress; d_{31} is the piezoelectric constant of the PZT when the stress is zero; $\overline{Y_{11}^E} = (1 + j\eta)Y_{11}^E$ is the elastic modulus of the PZT when the
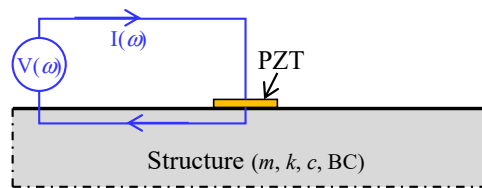

Fig. 1 The electro-mechanical interaction between target structure and PZT sensor

electric field is zero; η and δ are the damping loss factor of the structure and the dielectric loss factor of the PZT, respectively; $k = \omega\sqrt{\rho/\overline{Y_{11}^E}}$ is the number of wavelengths; ρ is the mass density of the PZT; l_p, w_p and t_p are the length, width and thickness of the PZT sensor, respectively.

If the structure is considered a one-degree-of-freedom system, then $Z_s(\omega)$ is expressed as

$$Z_s(\omega) = \frac{1}{j\omega}([K] + j\omega[C] - \omega^2 M) \tag{2}$$

Eq. (2) shows that the structure's mechanical impedance is a function of the dynamic characteristics such as mass (*m*), stiffness (*k*), and damping coefficient (*c*). Consequently, any change in the dynamic characteristics leads to a change in the EMI responses. The main principle of the impedance SHM method is to monitor the change in the structure's mechanical impedance responses due to damage. However, the structure's mechanical impedance is difficult to measure. In practice, the PZT sensor's electrical impedance is measured. According to Eq. (1), the electro-mechanical impedance $Z(\omega)$ is directly related to the structure's mechanical impedance $Z_s(\omega)$. When the structural damages occur, the mechanical impedance of the structure will change, and the EMI will change.

2.2 Impedance-based damage index

In impedance-based damage detection, the damages are represented by a change in the impedance responses measured from the PZT sensor. That change is quantified through statistical techniques. In this study, the RMSD (root mean square deviation) index based on the difference between the EMI responses of the two stages, before and after the presence of damage, is utilized. The RMSD index is determined as follows

$$RMSD = \sqrt{\frac{\sum_{i=1}^{n}[Z^*(\omega_i) - Z(\omega_i)]^2}{\sum_{i=1}^{n}[Z(\omega_i)]^2}} \tag{3}$$

where *n* is the number of data in the considered frequency range; $Z(\omega_i)$ is the EMI responses before the damage's presence of the ith frequency; $Z^*(\omega_i)$ is the EMI responses after the damage's presence of the ith frequency. In order to alarm the occurrence of damage, the following rule is performed. If the RMSD index is greater than 0, the structure is damaged; and vice versa, if the RMSD index is 0, no damage is present.

2.3 Artificial neural network

Multi-layer perceptron (MLP) artificial neural network model is widely used for engineering applications. A general MLP ANN is one with *k* layers (Fig. 2), with $k \geq 2$; usually, the input layer is not taken into account. As a result, the MLP ANN includes (*k*-1) hidden layer and an output layer (the kth layer). The general structure of the MLP ANN is as follows: input is a vector of (X_1, X_2, ..., X_n) in *n*-dimensional space, and output is a vector (Y_1, Y_2, ..., Y_m) in *m*-dimensional space. For classification problems, *m* is the number of classes to be classified, and *n* is the size of the input sample. Each neuron of the following layer is connected to all the neurons of the preceding
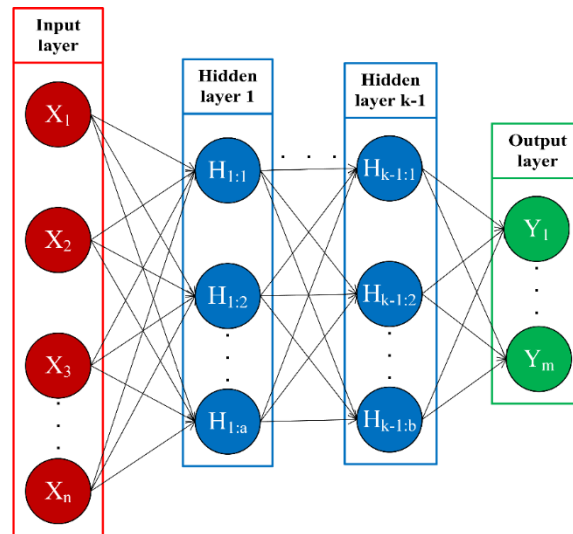
Fig. 2 Multi-layer perceptron artificial neural network model

layer. The neuron's output of the previous layer is the neuron's input of the next layer. The working way of the MLP ANN is as follows. The neurons in the input layer receive the signal and process it by summing the weights, send it to the transfer function, and then output the result. This result is transmitted to the neurons of the first hidden layer. The neurons here receive input signals, process, and send the results to the second hidden layer. The process continues until the neurons of the output layer give the result.

2.4 Proposed damage detection method

In this study, a structural damage identification method using impedance responses and MLP ANN is proposed. This method is capable of identifying the damage's occurrence, location, and extent. First, the impedance responses are divided into sub-frequency ranges with the same range width. Next, the RMSD index is calculated for each sub-frequency range. As a result, the occurrence of damage is alarmed, and the sensitivity of each sub-frequency range to damage is determined. The impedance responses of the most sensitive sub-frequency range are fed into the MLP ANN for training and predicting. Using the MLP ANN, in essence, can be understood as having a set of input values X that will map out a set of Y values through the transfer function f as follows

$$Y = f\left(\sum_{i}^{n} W_i X_i + b\right) \tag{4}$$

The result of the transfer function depends on the input value X_i, the weight set W_i, and the threshold value b. A neural network that wants to be predicted must go through a training phase to find the most suitable W_i and b values. The sub-frequency range that has high and clear resonant impedance peak and has a change in RMSD index is considered to be the most sensitive sub-frequency range to structural damage. Therefore, the impedance responses of this range will be used as input to the MLP ANN to predict the location and extent of the damage.

3. Numerical verification

3.1 Finite element model and impedance responses

Finite element (FE) software, ANSYS, featuring electro-mechanical impedance simulation, was used to simulate an aluminum beam with free boundary conditions (Fig. 3). In the FE model, the SOLID185 element was used for the beam, and the SOLID5 element was used for the PZT sensor.

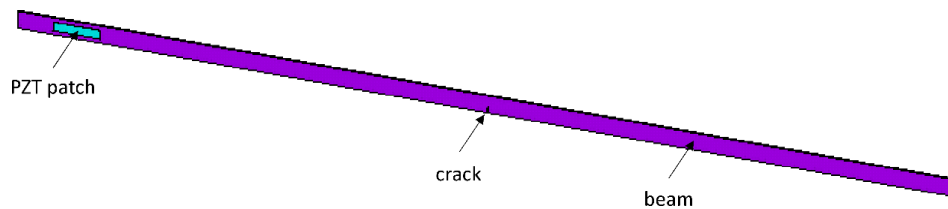
Fig. 3 Aluminum beam (Liu and Jiang 2009)

Fig. 4 FE model of the aluminum beam

Table 1 Material properties of the aluminum beam

Property	Symbol	Value
Elastic modulus (N/m^2)	E	72.5E9
Mass density (kg/m^3)	ρ	2700
Poisson's ratio	v	0.345

Table 2 Material properties of the PZT sensor

Property	Symbol	Value
Mass density (kg/m^3)	ρ	7650
Elasticity constant (N/m^2)	$C_{11} = C_{22}$	9.74E10
	C_{12}	5.03E10
	$C_{13} = C_{23}$	4.73E10
	C_{33}	7.93E10
	C_{44}	2.35E10
	$C_{55} = C_{66}$	1.90E10
Piezoelectric stress coefficients (C/m^2)	e_{31}	-8.70279
	e_{33}	17.56576
	e_{15}	14.411
Electrical permittivity (F/m)	$\varepsilon_{11} = \varepsilon_{22}$	9.164E-9
	ε_{33}	6.906E-9

In order to verify the accuracy of the numerical simulation, impedance responses from the FE model were compared with the corresponding results of Liu and Jiang (2009).

The FE model of the aluminum beam is completely similar to the data of Liu and Jiang (2009) (Fig. 4, Table 1, Table 2). The aluminum beam sample has dimensions of 1000 × 20 × 2 mm. The PZT sensor having dimensions of 50×10×0.5 mm is placed at a distance of 62.5 mm from the left end of the beam. A crack is created with two lengths of 3 mm and 6 mm at a position of 500 mm from the beam's left end. The excitation voltage for the PZT sensor was 4 V. The numerical simulation was performed with three cases: aluminum beam without crack, aluminum beam with a crack of 3 mm, and aluminum beam with a crack of 6 mm. The frequency range was considered
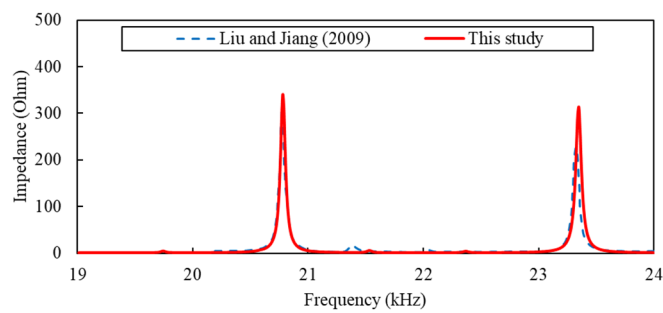

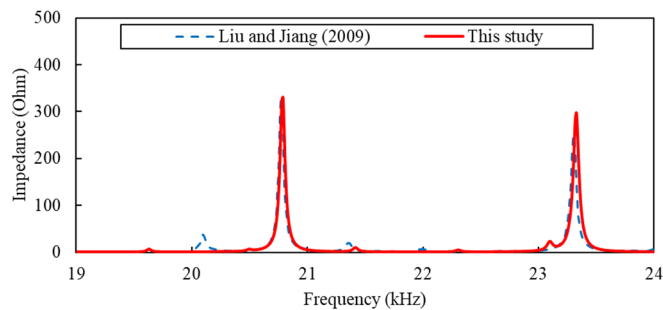Fig. 5 EMI responses of the aluminum beam without crack

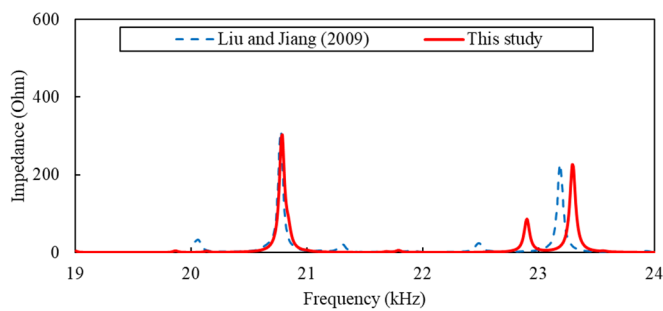Fig. 6 EMI responses of the aluminum beam with a crack of 3 mm

Fig. 7 EMI responses of the aluminum beam with a crack of 6 mm

Table 3 Comparison of impedance resonant peaks

Case	The first peak			The second peak		
	Liu and Jiang (2009) (kHz)	This study (kHz)	Difference (%)	Liu and Jiang (2009) (kHz)	This study (kHz)	Difference (%)
No crack	20.78	20.78	0.0	23.32	23.35	0.1
Crack of 3 mm	20.77	20.78	0.0	23.30	23.33	0.1
Crack of 6 mm	20.78	20.79	0.0	23.19	23.30	0.5

19 – 24 kHz. Figs. 5-7 show the comparison of impedance responses between Liu and Jiang (2009) and this study.

For each case, the number of frequency peaks from this study is the same as Liu and Jiang (2009). The cases of without crack and crack of 3 mm are two peaks, the case of crack of 6 mm is three peaks. However, there are two resonant peaks for all three cases. The impedance peaks in this study tend to deviate to the right from Liu and Jiang (2009)'s peaks, with a negligible deviation of less than 1% (Table 3). From the comparison, this study shows high accuracy and reliability in simulation for impedance responses. Therefore, the numerical simulation results are used for the problem of crack detection in the structure.

3.2 Crack detection results

In section 3.1, the aluminum beam simulated by ANSYS software has demonstrated the feasibility and reliability of impedance responses. In this section, an extensive study was performed to detect cracks in the beam. For the impedance-based damage detection, the selection of frequency range is important. Several studies have proven that the resonant impedance features are the most sensitive to structure damage. According to Ryu *et al*. (2017), the impedance responses were measured in the frequency range of 10 – 55 kHz; and the range with the highest frequency peak was 24 – 26 kHz. According to Ai *et al*. (2018), the impedance responses were measured in the frequency range of 0 – 300 kHz; and the range with the highest frequency peak was 130 – 290 kHz. However, the RMSD indexes were determined for the entire frequency range (i.e. 10 – 55 kHz for Ryu *et al*. (2017), and 0 – 300 kHz for Ai *et al*. (2018)). This reduces the sensitivity of the RMSD index to damage. In this study, the impedance responses were investigated in the cases: no crack, crack of 3 mm, and crack of 6 mm in the frequency range of
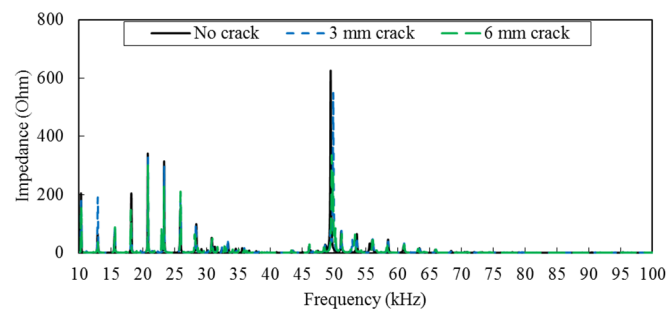

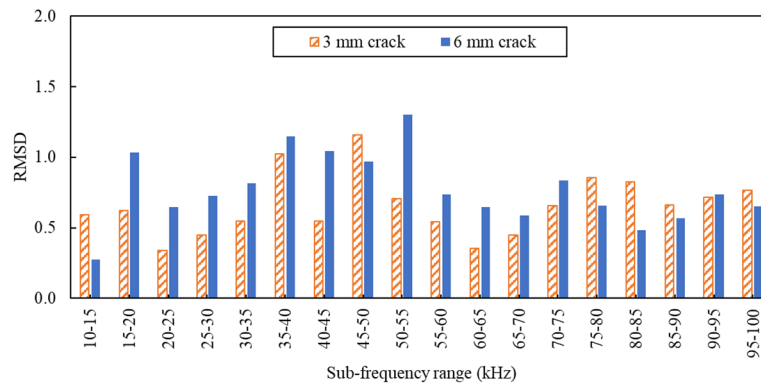Fig. 8 EMI responses of the aluminum beam in 10 – 100 kHz

Fig. 9 RMSD index for sub-frequency ranges

10 – 100 kHz, with a frequency step of 0.1 kHz. Fig. 8 shows the impedance responses from the simulation of three investigated cases. It should be noted that there were many impedance peaks with different magnitudes in this frequency range. Then, the impedance responses were divided into 18 sub-frequency ranges with a width of 5 kHz (i.e., 10 – 15 kHz, …, 95 – 100 kHz). The RMSD index was calculated according to Eq. (3) for 18 sub-frequency ranges. The results are shown in Fig. 9. As a result, the most sensitive sub-frequency range was selected to be the input data for the MLP ANN in the next step.

For the different sub-frequency ranges, the RMSD index is different in the same damage case. Furthermore, the different damage cases have different RMSD indexes in the same sub-frequency range. The RMSD index varies without a specific rule; for example, in the sub-frequency range of 10 – 15 kHz, the RMSD index decreases as the size of the crack increases; while in the sub-frequency range of 15 – 20 kHz, the RMSD index increases as the size of the crack increases. In the frequency range of 45 – 55 kHz, the RMSD index reaches the highest value, outperforming the rest of the sub-frequency ranges. Moreover, this is also the frequency domain with the highest resonant impedance peak in the impedance responses (Fig. 8). As a result, the crack's occurrence in the beam is successfully alarmed by the RMSD index. However, the RMSD index cannot identify the size of the cracks. Therefore, the MLP ANN is employed to determine the crack size in the beam.

In this study, two more crack cases, a crack of 2 mm and a crack of 5 mm, were proposed for the problem of predicting the size of the crack. Thus, the training cases were no crack, crack of
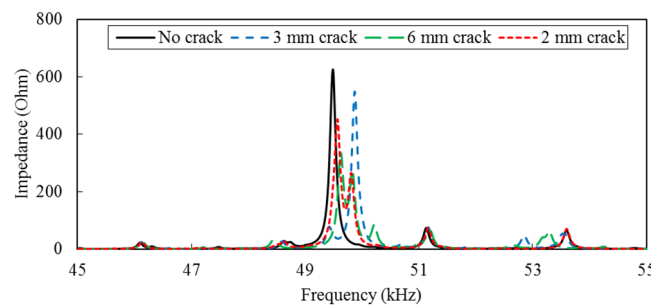

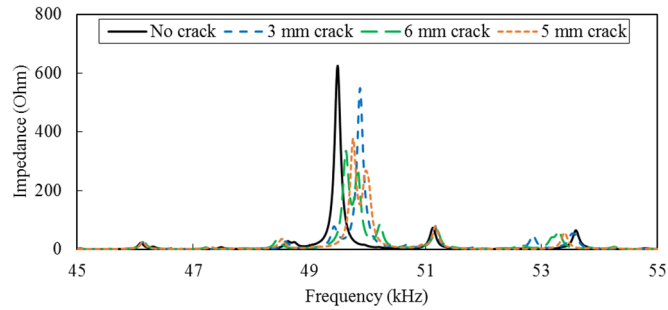Fig. 10 EMI responses for prediction case of 2 mm crack

Fig. 11 EMI responses for prediction case of 5 mm crack

Table 4 Crack size prediction results by the MLP ANN

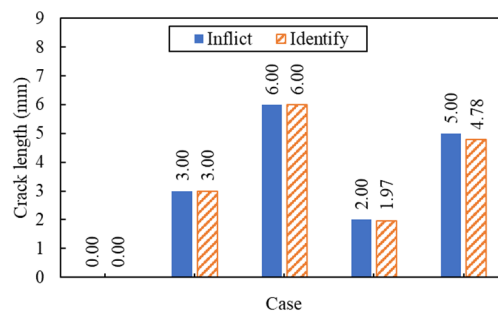| Data type	Inflicted crack (mm)	Identified crack (mm)	Error (%)
Training	0.00	0.00	-
Training	3.00	3.00	0.00
Training	6.00	6.00	0.00
Prediction	2.00	1.97	1.50
Prediction	5.00	4.78	4.40

Fig. 12 Crack size prediction results by the MLP ANN

3 mm, and crack of 6 mm; the predicting cases were crack of 2 mm, and crack of 5 mm. The frequency range of 45 – 55 kHz, with a frequency step of 0.01 kHz, was used for the problem. Figs. 10-11 show the impedance responses which were also the input data for the MLP ANN. The results of crack size identification are summarized in Table 4 and Fig. 12. For the training cases, the accuracy of crack size identification results is 100%. For the prediction cases, the accuracy of crack size identification results is 98.5% for crack of 2 mm case, and 95.6% for crack of 5 mm case. Thus, the size of the crack is successfully identified with very high accuracy by the MLP ANN.

4. Multiple cracks detection using the proposed MLP ANN

After successfully identifying the crack's occurrence and size of the single crack problem, the feasibility of the proposed method is verified by an extended study of the multiple cracks problem. An aluminum beam sample of the same size and material properties as section 3 is examined. Two PZT sensors (i.e., PZT 1 and PZT 2) which have dimensions of $50 \times 10 \times 0.5$ mm are placed at distances of 62.5 mm and 462.5 mm from the left end of the beam. The material properties of the PZT sensors are the same as section 3. Two cracks (i.e., crack 1 and crack 2) are created at the positions of 100 mm and 500 mm from the beam's left end. Fig. 13 illustrates the aluminum beam's schematic diagram. Table 5 lists the crack scenarios which include six different cases. A FE model of the beam was established. The impedance responses were investigated in the frequency range of 10 – 100 kHz, with a frequency step of 0.1 kHz. As shown in Fig. 14, the impedance responses have the highest resonant impedance peaks in the range of 45 – 55 kHz for both the PZT 1 and the PZT 2. Thus, the results of the impedance responses are similar to section 3; especially, for the PZT 1. Then, the impedance responses were divided into 18 sub-frequency ranges with a width of 5 kHz (i.e., 10 – 15 kHz, …, 95 – 100 kHz). As a result, the effective frequency range of 45 – 55 kHz was selected to be the input data for the MLP ANN.

For the MLP ANN, the training cases were from case 1 to case 5; the predicting case was case 6 which includes two cracks of different sizes. It should be noted that the PZT 1 was placed near crack 1, and the PZT 2 was placed near crack 2. The frequency range of 45 – 55 kHz, with a frequency step of 0.01 kHz, was used for the problem. Figure 15 shows the impedance responses which were also the input data for the MLP ANN. The results of crack size identification are summarized in Table 6 and Fig. 16. For the training cases with a single crack, the accuracy of crack size identification results is over 95%. This also means that the location of the crack is precisely determined. For the prediction case with the multiple cracks, the accuracy of crack size identification results is 99.0% for crack 1 and 96.5% for crack 2. Thus, the size of the two cracks is successfully predicted with very high accuracy by the MLP ANN.
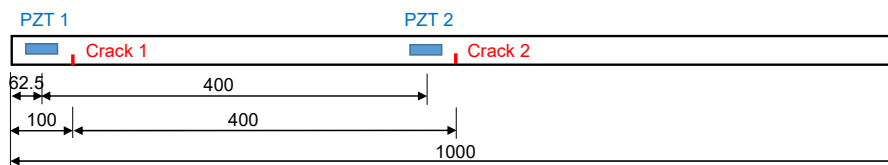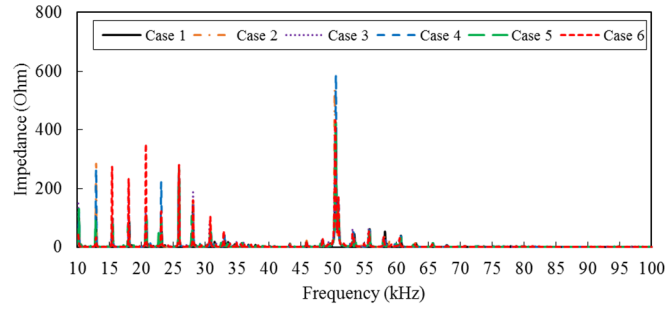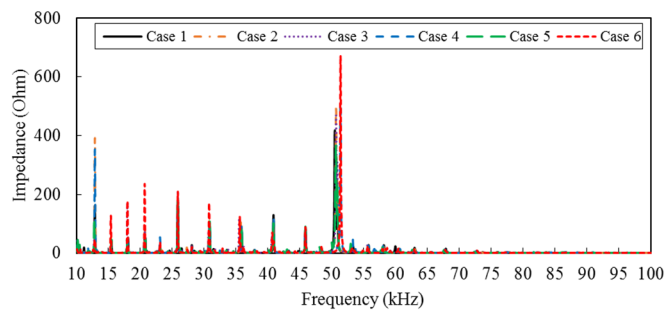

Fig. 13 Schematic diagram of the aluminum beam for the multiple cracks problem

Table 5 Crack scenarios for the multiple cracks problem

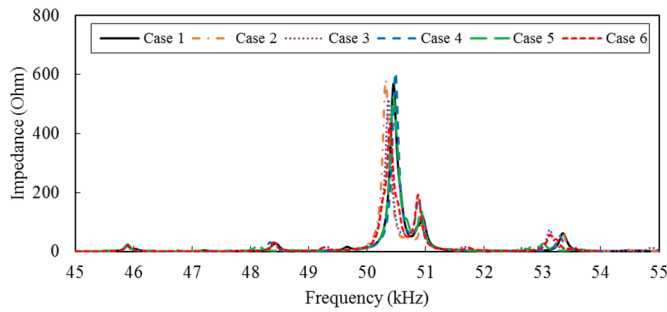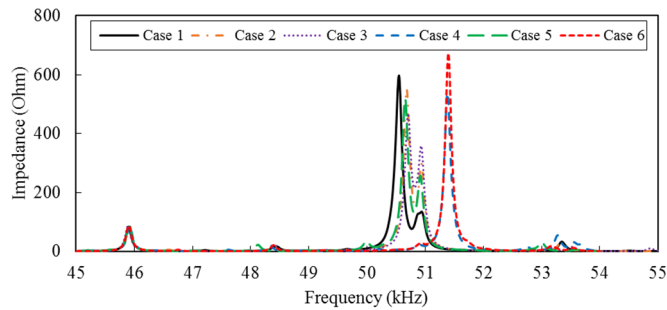| Case	Crack 1 (mm)	Crack 2 (mm)
1	0.00	0.00
2	3.00	0.00
3	6.00	0.00
4	0.00	3.00
5	0.00	6.00
6	5.00	2.00

(a) PZT 1

(b) PZT 2

Fig. 14 EMI responses in 10 – 100 kHz for the multiple cracks problem

(a) PZT 1

(b) PZT 2

Fig. 15 EMI responses in 45 – 55 kHz for the multiple cracks problem

Table 6 Crack size prediction results for the multiple cracks problem

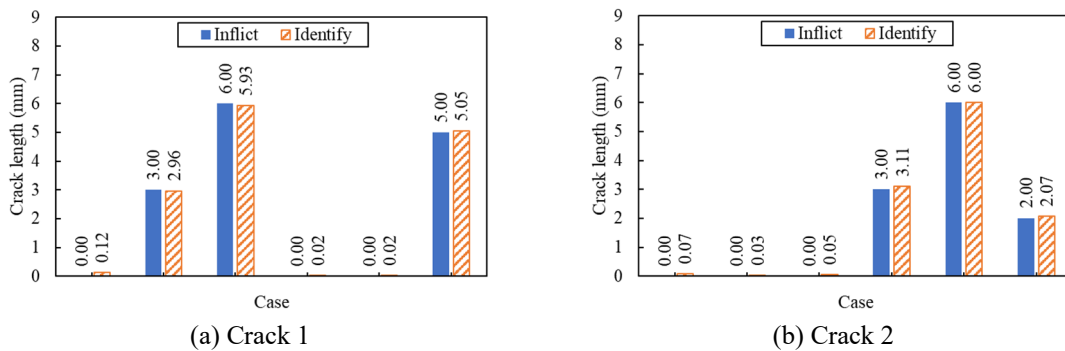| Case	Data type	Crack 1			Crack 2		
		Inflicted crack (mm)	Identified crack (mm)	Error (%)	Inflicted crack (mm)	Identified crack (mm)	Error (%)
1	Training	0.00	0.12	-	0.00	0.07	-
2	Training	3.00	2.96	1.33	0.00	0.03	-
3	Training	6.00	5.93	1.17	0.00	0.05	-
4	Training	0.00	0.02	-	3.00	3.11	3.67
5	Training	0.00	0.02	-	6.00	6.00	0.00
6	Prediction	5.00	5.05	1.00	2.00	2.07	3.50

(a) Crack 1   (b) Crack 2

Fig. 16 Crack size prediction results for the multiple cracks problem

5. Conclusions

This paper proposed a nondestructive method to detect cracks in metal structures by using a combination of electro-mechanical impedance responses and artificial neural networks. Firstly, the theories of impedance responses and impedance-based damage detection methods were briefly outlined. Secondly, the reliability of numerical simulations for impedance responses was demonstrated by comparing to pre-published results for an aluminum beam. Thirdly, the proposed method was used to detect cracks in the beam. The RMSD index was used to alarm the occurrence of the cracks, and the MLP ANN was employed to identify the size of the cracks. The selection of the effective frequency range was also investigated. The proposed method successfully and accurately identified the cracks' occurrence, location, and size in the structures. The main conclusions have been drawn as follows:

(1) The numerical simulation of EMI responses for the aluminum beam was successfully performed. The impedance responses from the FE model were in good agreement with the pre-published results.
(2) The crack's occurrence in the structure was successfully alarmed by the RMSD index. The RMSD index had a different sensitivity to damage depending on the frequency range.
(3) The crack's location and size in the structure were accurately identified by the MLP ANN. The results show that the accuracy of the crack size detection was over 95%.

The method of this study can be applied to identify the occurrence, location, and size of a single crack, multiple cracks in metal structures. However, the impedance response is local sensing, so multiple PZT sensors must be used to detect multiple cracks. Therefore, this study can serve as the foundation for further studies; especially for the civil structures.

Acknowledgments

References

Ai, D., Luo, H., Wang, C. and Zhu, H. (2018), "Monitoring of the load-induced RC beam structural tension/compression stress and damage using piezoelectric transducers", *Eng. Struct.*, **154**, 38-51. https://doi.org/10.1016/j.engstruct.2017.10.046

Avci, O., Abdeljaber, O., Kiranyaz, S., Hussein, M., Gabbouj, M. and Inman, D.J. (2021), "A review of vibration-based damage detection in civil structures: From traditional methods to Machine Learning and Deep Learning applications", *Mech. Syst. Signal Process.*, **147**(107077), 1-45. https://doi.org/10.1016/j.ymssp.2020.107077

Fan, X., Li, J. and Hao, H. (2021), "Review of piezoelectric impedance based structural health monitoring: Physics-based and data-driven methods", *Adv. Struct. Eng.*, **24**(16), 3609-3626. https://doi.org/10.1177/13694332211038444

Farrar, C.R. (2001), "Historical overview of structural health monitoring", Lecture Notes on Structural Health Monitoring Using Statistical Pattern Recognition; Los Alamos Dynamics, Los Alamos, NM, USA.

Giurgiutiu, V. and Zagrai, A. (2005), "Damage detection in thin plates and aerospace structures with the electro-mechanical impedance method", *Struct. Health Monitor.*, **4**(2), 99-118. https://doi.org/10.1177/1475921705049752

Ho, D.D., Ngo, T.M. and Kim, J.T. (2014), "Impedance-based damage monitoring of steel column connection: numerical simulation", *Struct. Monitor. Maint., Int. J.*, **1**(3), 339-356. https://doi.org/10.12989/smm.2014.1.3.339

Ho, D.D., Huynh, T.C., Luu, T.H.T. and Le, T.C. (2021), "Electro-mechanical impedance-based prestress force monitoring in prestressed concrete structures", In: *Structural Health Monitoring and Engineering Structures*, **148**, 413-423. https://doi.org/10.1007/978-981-16-0945-9_33

Huynh, T.C., Dang, N.L. and Kim, J.T. (2017), "Advances and challenges in impedance-based structural health monitoring", *Struct. Monitor. Maint., Int. J.*, **4**(4), 301-329. https://doi.org/10.12989/smm.2017.4.4.301

Lee, J.J., Yun, C.B., Lee, J.W. and Jung, H.Y. (2005), "Neutral network-based damage detection for bridges considering errors in baseline finite element model", *J. Sound Vib.*, **280**, 555-578. https://doi.org/10.1016/j.jsv.2004.01.003

Li, H.N., Yi, T.H., Ren, L., Li, D.S. and Huo, L.S. (2014), "Reviews on innovations and applications in structural health monitoring for infrastructures", *Struct. Monitor. Maint., Int. J.*, **1**(1), 1-45. https://doi.org/10.12989/smm.2014.1.1.001

Liang, C., Sun, F.P. and Rogers, C.A. (1994), "Coupled electro-mechanical analysis of adaptive material systems-determination of the actuator power consumption and system energy transfer", *J. Intell. Mater. Syst. Struct.*, **5**, 12-20. https://doi.org/10.1177/1045389X9400500102

Liu, X. and Jiang, Z. (2009), "Design of a PZT patch for measuring longitudinal mode impedance in the assessment of truss structure damage", *Smart Mater. Struct.*, **18**(125017). https://doi.org/10.1088/0964-1726/18/12/125017

Min, J., Park, S., Yun, C.B., Lee, C.G. and Lee, C. (2012), "Impedance-based structural health monitoring incorporating neural network technique for identification of damage type and severity", *Eng. Struct.*, **39**, 210-220. https://doi.org/10.1016/j.engstruct.2012.01.012

Nguyen, T.T., Phan, T.T.V., Ho, D.D., Pradhan, A.M.S, and Huynh, T.C. (2022), "Deep learning-based autonomous damage-sensitive feature extraction for impedance-based prestress monitoring", *Eng. Struct.*, **259**(114172), 1-18. https://doi.org/10.1016/j.engstruct.2022.114172

Park, G., Sohn, H., Farrar, C. and Inman, D. (2003), "Overview of piezoelectric impedance-based health monitoring and path forward", *Shock Vib. Digest*, **35**, 451-463.

Park, S., Ahmad, S., Yun, C.B. and Roh, Y. (2006), "Multiple crack detection of concrete structures using impedance-based structural health monitoring techniques", *Experim. Mech.*, **46**(5), 609-618. https://doi.org/10.1007/s11340-006-8734-0

Rao, A.S., Nguyen, T., Palaniswami, M. and Ngo, T. (2021), "Vision-based automated crack detection using convolutional neural networks for condition assessment of infrastructure", *Struct. Health Monitor.*, **20**(4), 2124-2142. https://doi.org/10.1177/1475921720965445

Ryu, J.Y., Huynh, T.C. and Kim, J.T. (2017), "Experimental investigation of magnetic-mount PZT-interface for impedance-based damage detection in steel girder connection", *Struct. Monitor. Maint.*, *Int. J.*, **4**(3), 237-253. https://doi.org/10.12989/smm.2017.4.3.237

Sun, F.P., Chaudhry, Z., Liang, C. and Rogers, C.A. (1995), "Truss structure integrity identification using PZT sensor-actuator", *J. Intell. Mater. Syst. Struct.*, **6**, 134-139. https://doi.org/10.1177/1045389X9500600117

Yao, Y., Tung, S.T.E. and Glisic, B. (2014), "Crack detection and characterization techniques-An overview", *Struct. Control Health Monitor.*, **21**(12), 1387-1413. https://doi.org/10.1002/stc.1655

Zuo, C., Feng, X., Zhang, Y., Lu, L. and Zhou, J. (2017), "Crack detection in pipelines using multiple electromechanical impedance sensors", *Smart Mater. Struct.*, **26**(10). https://doi.org/10.1088/1361-665X/aa7ef

JK